

Karsten Dierks  
Matthias Dieckmann  
Dirk Niederstrasser  
Robert Schwartz  
Alfred Wegener

## Protein size resolution in human eye lenses by dynamic light scattering after in vivo measurements

Received: 22 July 1996  
Revised version received: 23 April 1997  
Accepted: 6 May 1997

K. Dierks  
Dierks+Partner System Technology,  
Pinneberger Weg 22+24,  
D-20257 Hamburg, Germany  
Tel. +44-40-8533010

M. Dieckmann  
ESA/ESTEC, Noordwijk, The Netherlands

D. Niederstrasser · R. Schwarz  
University Eye Clinic,  
Hamburg-Eppendorf, Germany

A. Wegener  
University Eye Clinic,  
Institute for Experimental Ophthalmology,  
Bonn, Germany

**Abstract** Dynamic light scattering (DLS) measurements were conducted with lowest intensity levels on human eye lenses ( $3.2 \text{ mW/cm}^2$ ) within measurement times of 3–5 s. A characterisation of the human eye under in-vivo conditions along the optical axis is given and a careful interpretation of the data is made, referring not only to in-vitro results of investigated solutions of lens chemistry and various crystallin fractions but also to measurements performed on intact human lenses under various scattering angles. The clinical study was expanded to 79

subjects with ages varying from 9 to 85 years with no serious diseases of the ocular lenses. A normalisation of Scheimpflug photography density data to the data obtained by DLS enables comparison of the two techniques and shows good agreement. The bimodal character of the viscoelastic properties of healthy eye lenses was confirmed; with an assumed viscosity of 2 cP, the mean size parameter of the smaller component is  $5.13 \pm 1.6 \text{ nm}$  and of the polymeric fraction 690 nm.

### Introduction

Lens transparency depends on special protein distributions in the lens fibre cells. Alterations in density, structural integrity and lens hydration lead to pathologic changes in refractive index and transparency which can result in the development of a cataract. The process of lens opacification is a complex phenomenon which has not been completely elucidated [8], although a classification of cataract types exists and some influencing factors have been demonstrated [2]. Conventional documentation of pathologic findings by slit-lamp microscopy is no longer sufficient to achieve the objective of better understanding. Even using the Scheimpflug technique, which is described by Hockwin [8], no statement about the molecular context can be made.

The technique of dynamic light scattering (DLS) has been commonly applied in colloidal chemistry for nearly 20 years [6]. First non-invasive in-vivo measurements by means of DLS were made by Tanaka and Ishimoto [14]. Benedek et al. determined visco-elastic lens properties

which corresponded to two protein radii of 3 nm and 90 nm in 1987 [9, 13], but optimal experimental conditions have only recently become available. A comprehensive overview of this technique, including results from the first in-vivo DLS measurements on ocular lenses, was given by Masters [10]. With this technique it is possible to look more closely at the molecular component and resolve the degree of polymerisation of the lens crystallins. In case of opacities, the refractive index increases rapidly along shortest pathlengths and this refractive index increment is the origin of stray light. The aggregation of lens proteins can be assumed responsible for the development of lens opacities. The DLS results must be carefully interpreted by considering the dimensional data of the lens crystallins. The molecular dimensions are described by White et al. [16], Taylor et al. [15], Chirgadze et al. [4] and Bax et al. [1].

### Materials and methods

The operation configuration of the used prototype of the lens protein size analyser LEPOSIA<sup>®</sup> and the underlying measurement and cal-

ulation principles are reported in [5]. With an appropriate interface it can be easily implemented into a Haag-Streit slit-lamp apparatus. With an intensity level of  $3.2 \text{ mW/cm}^2$  upon the retina, safe in-vivo measurements enable the resolution of various radii fractions. The brownian motion of suspended particles causes intensity fluctuations of the scattered light, if the stray light volume is enhanced by an incident light beam. These signal fluctuations are acquired by counting single photons and are analysed with an autocorrelator, which calculates the self-similarity of the recorded intensity fluctuations. The achieved intensity autocorrelation function (ACF) can be described as a superposition of exponential decays. The program CONTIN [12] was used for the conversion of the ACFs to decay time distributions. Under optimal instrumental conditions the amplitude of the ACF varies between 2 and 1. These values were closely approximated in our experiments. The time constant distribution of the exponential function corresponds to the relaxation properties of the investigated system and may be converted into sizes of the scattering centres, if their motion is diffusive. Usually this conversion is done by applying the Stokes-Einstein equation, but this is only justified if the diffusive character of the brownian motion can be verified. As indicated in [10], it is hardly possible to perform scattering vector-dependent measurements in vivo, but angle-dependent measurements with extracted eye lenses will elucidate this point and are described later. Throughout this article we use the term "size parameter" for the result of the Stokes-Einstein conversion, regardless of its applicability. In contrast to prior assumptions, it has been shown that particle sizing by DLS works even for concentrations up to 10% and is therefore suitable for measurements on human eye lenses [11].

This procedure has also been called photon correlation spectroscopy (PCS) as well. PCS, DLS and quasi-elastic light scattering (QELS) can be considered synonyms. The PCS instrumentation used for metabolism studies in earlier days was insufficient and led to incomplete conclusions [13]. The scattering angle used by LEPOSIA is  $160^\circ$ , comparable with the backscattering angle of approx.  $135^\circ$ , which corresponds to the observation direction of the illuminated lens slice in the specific camera geometry of the Scheimpflug camera used by Hockwin.

### Measurement procedures, lens system and sample preparation for in-vitro studies

Figure 1 shows both the side view of the lens (top) and the aspect from above (bottom). Human lens systems are examined with a conventional Haag-Streit slit lamp to which a light-pen-like optrode is attached by a mechanical system. This opto-mechanical system moves the scattering area of  $50 \mu\text{m} \times 0.5 \text{ mm}$  to any position within the lens. The standard procedure consists of several measurements in various positions of the lens along the optical axis (OA) (Fig. 1, 1). Precise positioning of the measurement volume in the eye lens, as needed, for example, for the determination of day-to-day changes in a given eye, is very difficult. Position repeatability was considered unnecessary if only data on change of aggregation of proteins were collected.

We differentiate posterior capsule (a), posterior subcapsular layer, posterior cortex and deep juvenile cortex (b), posterior nucleus (c), anterior nucleus (d), anterior adult and juvenile cortex to supranucleus layer (e) and cleft layer and anterior capsul (f).

In the outer parts of the lens parallel to the OA (1a), measurements in three layers have been made to prevent overlapping of scattering volumes. This procedure enables a comparison between DLS and Scheimpflug photography, the illuminated directions of which can be schematised by the planes parallel to the OA, (2) and (3).

The measurements were performed during a clinical study on 79 subjects.

The in-vitro experiments were carried out on some typical solutions of lens chemistry and on various crystallin fractions, obtained

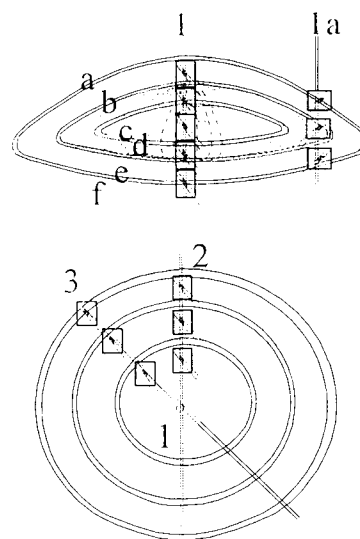


**Fig. 1** Schematic view of the measurement positions; the frames indicate the scattering centres with the illuminating and the received beam. See text for details

with electrophoretic separation. The cuvettes were examined with both techniques, DLS and Scheimpflug photography. Sample preparation after removal of the lens capsule and homogenisation were conducted according to Bours [3].

### Results of lens protein size analysis after a clinical in-vivo study

Due to the experience gained by measurements on highly concentrated protein solutions, a viscosity of 2 cP was found to be appropriate. The refractive index, applied for the calculations, was 1.38. With these values the Stokes-Einstein equation gives the size parameter directly from the decay times. In most cases the size parameter distributions were found to be bimodal. They consist of a small and a large component. An example of a typical ACF and the derived decay time distribution is given in Fig. 2.

For a purely diffusive motion of the molecules this size parameter equals the hydrodynamic radius of the molecules. In order to find out whether this is the case under experimental conditions, measurements on extracted eye lenses were performed under various scattering angles. This is, to the authors' knowledge, the first report of such measurements.

According to these tests, the small fraction seems to obey the theory of diffusive motion, because the angular dependence of the observed decay times for the small component corresponds to the theoretical expectation in the range of scattering angles from  $45^\circ$  to  $155^\circ$ , with a slightly worse agreement at small angles. Hence, in this case the size parameter can be interpreted as a molecular radius. The large component did not show a dependence

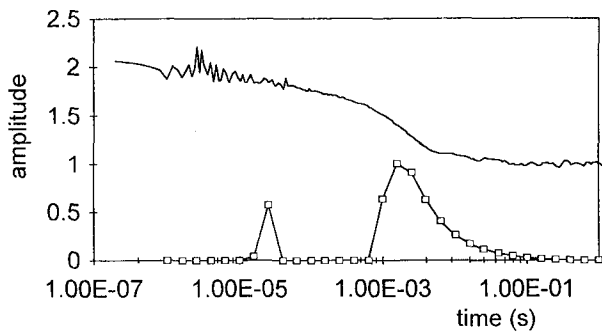


**Fig. 2** A typical autocorrelation function (*upper curve*) and the derived decay time distribution

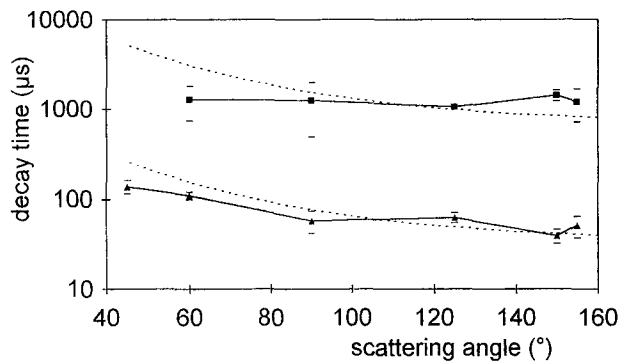


**Fig. 3** Measurement of decay time constants of the autocorrelation function as a function of scattering angle in an extracted human eye lens. The *squares* are the large component, while the *triangles* refer to the small component. The *dotted line* represents the theoretical value for a purely diffusive motion

of the decay time on the scattering angle. For the interpretation of the size parameter, this means the true radius of the large fraction is estimated to be only 30% of the calculated value, obtained from a simple conversion from decay time to radius values of the presumed crystallin aggregates. Their size parameter is meant as a first-order trial. The angle-dependent measurements are shown in Fig. 3.

The occurrence of the large components can be considered as caused by the aggregation or polymerisation tendencies of the crystallins. The protein parameter distributions of all patients with clear lenses and ages ranging from 20 to 60 years of age selected. The histogram in Fig. 4 shows the distribution of the smaller component, regarded as monomers.

The distribution of the large component for all ages with clear lenses is given in Fig. 5, using quasi-logarithmic bin sizes.

The size distribution of the aggregates itself may reveal a bimodal character in most of the investigated subjects with lens opacities. Figure 6 illustrates the conditions found in cataractous lenses.

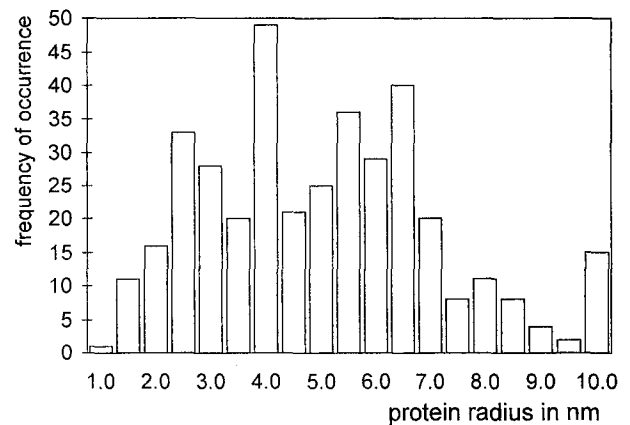


**Fig. 4** Histogram of the radius of the small component, measured in all positions in healthy eye lenses (mean size parameter  $5.13 \pm 1.6$  nm)

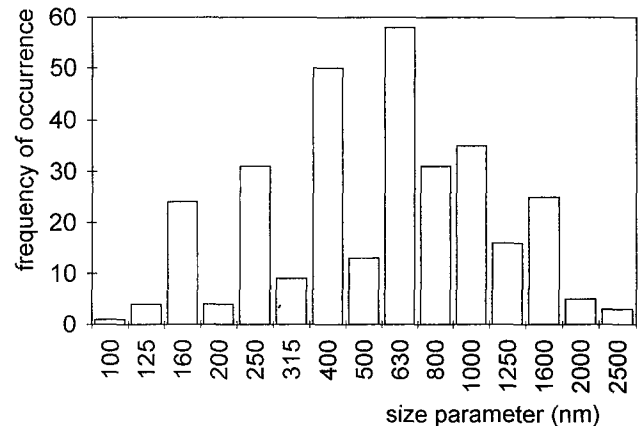


**Fig. 5** Size parameter histogram of the larger component, measured in all lens positions of the healthy eye lenses (mean size parameter  $690 \pm 470$  nm)

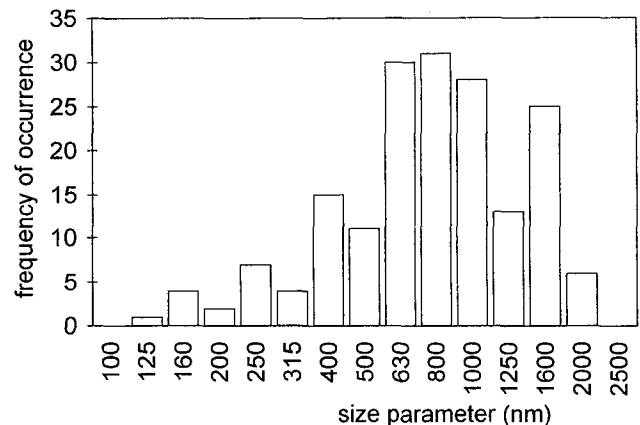


**Fig. 6** Size parameter histogram for the large component in cataractous eye lenses (mean size parameter  $880 \pm 460$  nm)

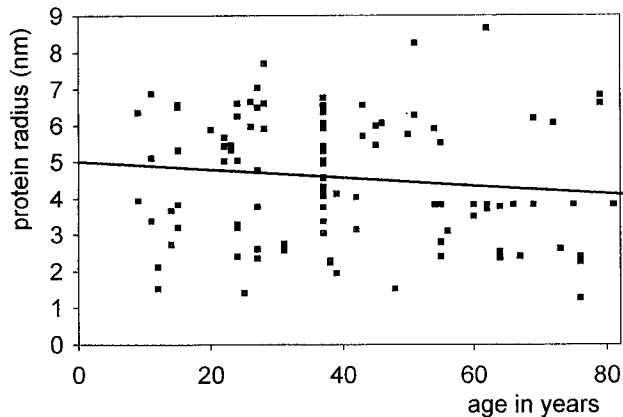


**Fig. 7** Radius of the small component as a function of age (nucleus only); the *solid line* is fitted to the data with intercept of  $5.0 \pm 0.38$  nm and a slope of  $0.01 \pm 0.009$ . No small component was found in the nucleus for volunteers over 80 years of age

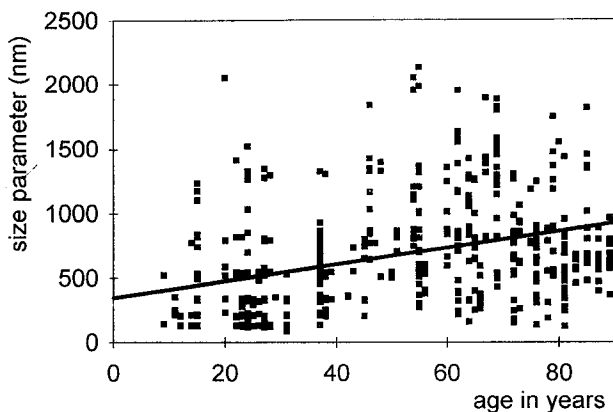


**Fig. 8** Size parameter for the large component as a function of age; the fitted line has an intercept of  $347 \pm 44$  and a slope of  $6.41 \pm 0.8$

### Correlograms and regression curves

According to earlier results, the monomeric radius seems to be correlated with the age of the subject, decreasing slightly with increasing age. This is not statistically significant, although examinations of the nucleus alone and of the entire lens show similar tendencies. The relationship is shown in Fig. 7.

The correlation between the polymeric component size parameter and the subject age is still positive and confirms earlier results, where a similar increase was found. Figure 8 shows the updated correlogram.

Figure 9 illustrates the ratio of the monomer distribution height to the aggregate distribution height, where the heights are taken as a measure for the relative amount of each fraction. It is determined by finding the ratio of the heights of the two peaks, and the obvious decrease of the small component indicates the reduction of the

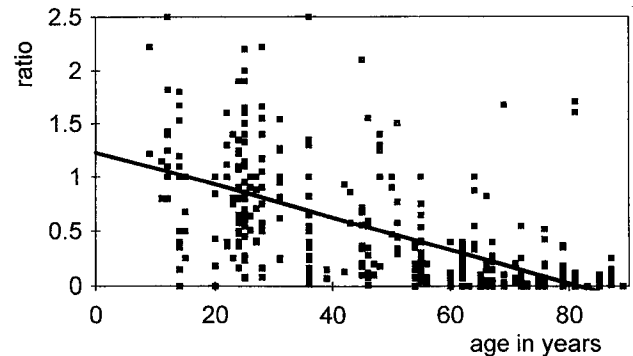


**Fig. 9** The relative decrease of the freely diffusing small component is shown as the ratio of the small to the large component as function of age (all lens positions); intercept of fit is  $1.23 \pm 0.05$  and the slope  $0.015 \pm 0.001$

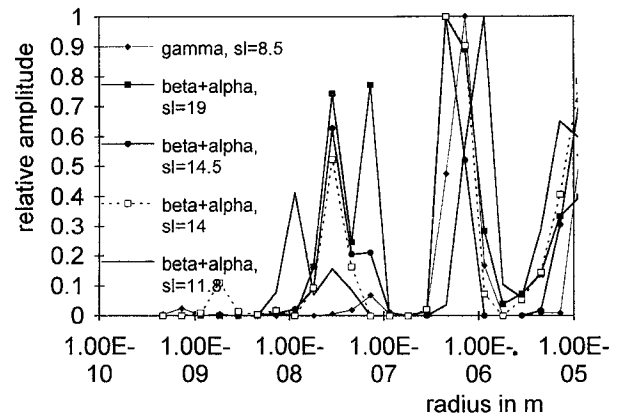


**Fig. 10** DLS and Scheimpflug data from bovine crystallin fractions after isoelectric focussing (*sl* scattered light intensity)

number of freely diffusing protein components in the lens cells of older subjects.

### In-vitro measurements

To compare in-vivo and in-vitro data, standard protein solutions and bovine crystallin preparations were placed in cuvettes. The cuvettes were measured by means of DLS and then photographed with the Scheimpflug camera. The radius distributions for the crystallin fractions and the scattered light intensity from the Scheimpflug camera are shown in Fig. 10.

Figure 11 illustrates the examination of the protein standards.

To analyse whether different concentrations and sample preparations influence the measurement results, several dilutions made. The results are presented in Fig. 12.

The results of these experiments support the assumption that the scattering observed with both techniques is

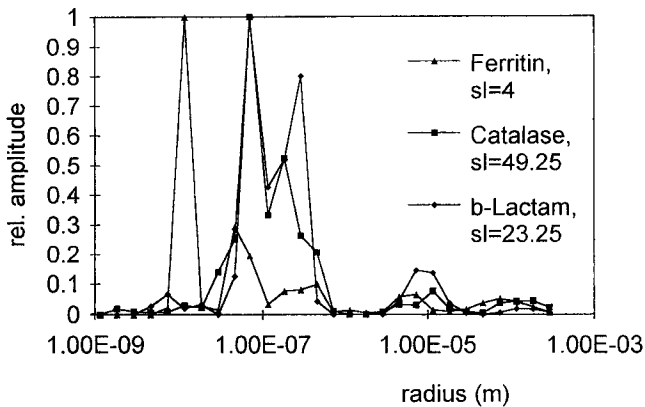


**Fig. 11** DLS and Scheimpflug measurements on standard protein solutions (conc. 5 g/l)

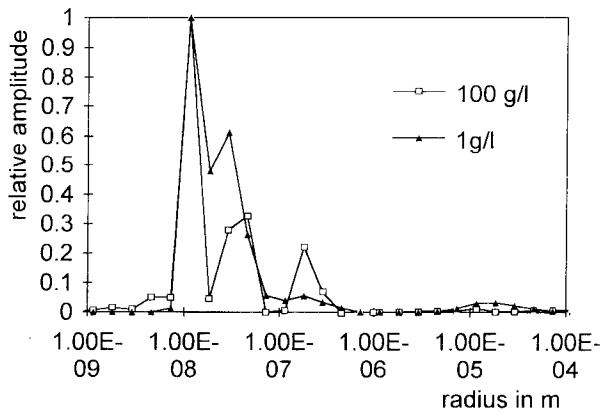


**Fig. 12** Concentration dependence of DLS measurements of bovine crystallin solutions (all water-soluble crystallins from the whole bovine lens)

caused by the lens proteins and their aggregates. Cell organelles and membranes as a source of light scattering can be excluded.

The sample preparation yields different data *in vivo* (unseparated) and *in vitro* (separated).

### Correction of light attenuation for Scheimpflug densitometries

The incident light and the scattered light is attenuated on its path through the lens, and this attenuation is expected to describe an exponential decay as a function of depth in the lens. Since the lens is an inhomogeneous structure, this approach could only be regarded as a first approximation, but in order to obtain densities independent of the position in the lens, the light attenuation must be corrected. This is done by an exponential fit curve as shown in Fig. 13, which is afterwards subtracted from each measured density curve. A constant  $A$  is then added in order

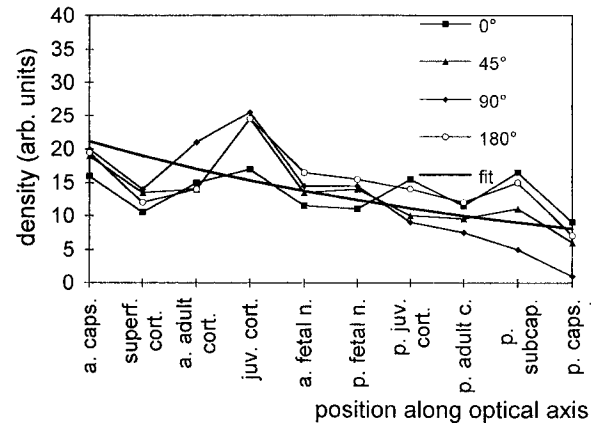


**Fig. 13** Typical Scheimpflug density curves, measured at different angles of the illumination plane and the fitted exponential function (solid line). *a. caps.* Anterior capsule, *superf. cort.* superficial cortex, *a. adult cort.* anterior adult cortex, *juv. cort.* juvenile cortex, *a. fetal n.* anterior fetal nucleus, *p. fetal n.*, posterior fetal nucleus, *p. juv. cort.* posterior juvenile cortex, *p. adult c.* posterior adult cortex, *p. subcap.* posterior subcapsular layer, *p. caps.* posterior capsule

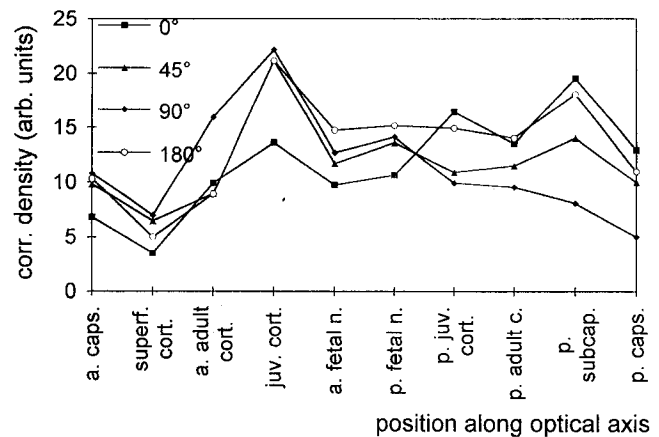


**Fig. 14** Corrected densities obtained from Fig. 13

to avoid negative values;  $A$  is chosen in a way that the average density value remains unchanged. The result is depicted in Fig. 14.

### Normalisation of Scheimpflug photography to lens protein size parameter analysis

To make the Scheimpflug data comparable with the DLS measurements, the densities had to be corrected by multiplication with a constant  $B$ . The corrected relative densities and the polymeric size data show good agreement, as indicated in Fig. 15, where superposition of the two curves is used to illustrate this approximative normalisation. The derived error corridors are included in this figure.

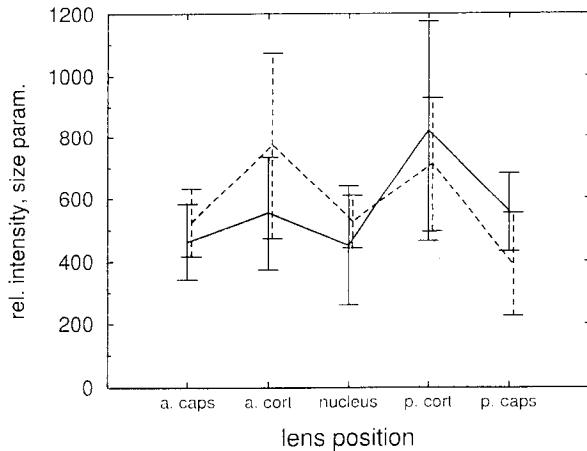


**Fig. 15** Scheimpflug densitometric data (dotted line) and protein size parameter obtained with DLS (solid line)

## Conclusion

The experiments show that DLS is a useful complement to the Scheimpflug technique, providing insight into the molecular dimensions under in-vitro conditions.

Taking into account that the hydrated crystallin molecule increases in its dimension, the DLS measurements

support the published X-ray data on the dehydrated monomer.

An optimised DLS instrument was realized, and more precise resolution of two protein size classes in clear lenses as a function of lens position was achieved. After enlargement of the clinical study to 79 subjects and more careful interpretation especially of the larger fraction, the radius of the smaller fraction can be given as 5.13 nm with a standard deviation of 1.6 nm. Referring to the cuvette experiments, this fraction corresponds very likely to the monomers or oligomers of the human eye crystallins. For the polymeric component a size parameter value of 690 nm, with a broad distribution, was observed. A preliminary scale factor of 30% was introduced in order to convert this value into aggregate radii.

The decrease of the small component in old lenses is quantified by DLS and may reflect the loss of  $\gamma$ -crystallin, observed by Hockwin [7], compared to conditions encountered during youth. This decrease may cause the observed increase of protein aggregate sizes, which are transferred into quantified values as well.

Application of the presented techniques, accompanied by detailed analysis, will be necessary for a closer look at the aetiology of many types of cataract formation. Cataract prevention and the development of corresponding medication will very likely profit from the DLS measurement technique.

## References

- Bax B, Lapatto R, Nalini V, Driessen H, Lindley PF, Mahadevan D, Blundell TL, Slingsby C (1990) Analysis of B2-crystallin and evolution of oligomeric lens proteins. *Nature* 347:776-779
- Benedek GB (1984) The molecular basis of cataract formation. *Ciba Found Symp* 106:237-247
- Bours J (1980) Species specificity of the crystallins and the albuminoid of the aging lens. *Comp Biochem Physiol* 65B:215-222
- Chirgadze XYU, Nevsak N, Vernolova E, Nikonov S, Sergeev YU, Brazhinkov E, Femnkova M, Linin V, Urzhumtsev A (1991) Crystal structure of calf lens gamma-crystallin IIb at 2.5 angstrom resolution: its relation to function. *Exp Eye Res* 53:295-304
- Dierks K, Dieckmann M (1994) Diagnostic methods and tissue parameter investigations together with measurement results (in vivo). *Proceedings of Biomedical Optics, SPIE OE/LASE '94, Ophthalmic Technologies IV*:2126-2143
- Ford NC (1985) Light scattering apparatus. In: Pecora R (ed) *Dynamic light scattering*. Plenum Press, New York
- Hockwin O (1989) Die Scheimpflug-Photographie der Linse. *Fortschr Ophthalmol* 86:304-311
- Hockwin O (1993) Biochemie der Augenlinse. *Klin Monatsbl Augenheilkd* 202:544-551
- Libondi T, Magnante P, Chylack LT, Benedek GB (1986) In vivo measurement of the aging rabbit lens using quasielastic light scattering. *Curr Eye Res* 5:411-419
- Masters BR (1990) *Noninvasive diagnostic techniques in ophthalmology*. Springer, New York Berlin Heidelberg, pp 342-365
- Meyer WV et al. (1996) A single wavelength cross-correlation technique which suppresses multiple scattering. In: *Photon correlation and scattering*, OSA Tech Digest Ser (Optical Society of America) 14:104-107
- Provencher SW (1982) A general purpose constrained regularization program for inverting noisy non-linear algebraic and integral equations. *Comput Phys Comm* 27:229-242
- Tanaka T, Benedek GB (1975) Observation of protein diffusivity in intact human and bovine eye lenses with application to cataract. *Invest Ophthalmol* 6:449-456
- Tanaka T, Ishimoto C (1977) In vivo observation of protein diffusivity in rabbit lenses. *Invest Ophthalmol* 16:135
- Taylor WR, Thornton JM, Turner WG (1983) Structure resolution of II-crystallin. *J Mol Graphics* 1:30-38
- White HE, Driessen HPC, Slingsby C, Moss DS, Lindley PF (1989) Packing interaction in the eye-lens: structural analysis, internal symmetry and lattice interactions in the bovine IVa-crystallin. *J Mol Biol* 207:217-235